frontiers | Frontiers in Marine Science

TYPE Original Research
PUBLISHED 12 January 2024
DOI 10.3389/fmars.2023.1269411

OPEN ACCESS

EDITED BY
Andrew R Thurber,
Oregon State University, United States

REVIEWED BY
Guoyong Yan,
Hong Kong University of Science and Technology, China
Taewoo Ryu,
Okinawa Institute of Science and Technology Graduate University, Japan

*CORRESPONDENCE
Yuefeng Cai
yuefengcai@jou.edu.cn
Xin Shen
shenthin@163.com

†These authors have contributed equally to this work and share first authorship

RECEIVED 30 July 2023
ACCEPTED 28 December 2023
PUBLISHED 12 January 2024

CITATION
Mao N, Shao W, Cai Y, Kong X, Ji N and Shen X (2024) Comparative omics analysis of a new deep-sea barnacle species (Cirripedia, Scalpellomorpha) and shallow-water barnacle species provides insights into deep-sea adaptation. *Front. Mar. Sci.* 10:1269411. doi: 10.3389/fmars.2023.1269411

Comparative omics analysis of a new deep-sea barnacle species (Cirripedia, Scalpellomorpha) and shallow-water barnacle species provides insights into deep-sea adaptation

Ning Mao[1,2†], Wentai Shao[1,2†], Yuefeng Cai[1,2*], Xue Kong[1,2], Nanjing Ji[1,2] and Xin Shen[1,2*]

[1]Jiangsu Key Laboratory of Marine Bioresources and Environment, Jiangsu Key Laboratory of Marine Biotechnology, Jiangsu Ocean University, Lianyungang, China, [2]Co-Innovation Center of Jiangsu Marine Bio-Industry Technology, Jiangsu Ocean University, Lianyungang, China

Barnacles have demonstrated adaptability to a range of habitats, spanning from shallow water to the deep sea. Given the harsh conditions present in hydrothermal vents, hydrothermal vent barnacles serve as the model organism for investigating the interplay between evolution and adaptability. In order to gain insights into barnacle adaptive characteristics, particularly within hydrothermal vents, we conducted a comprehensive analysis of the mitogenomes and transcriptome in a deep-sea barnacle (*Vulcanolepas fijiensis*), in comparison to its shallow-water related species. The mitogenomes with the same genetic skews and the non-synonymous/synonymous mutation ratios (K_a/K_s) of the mitogenomes indicate that the protein-coding genes (*COIII*, *ND2*, and *ND6*) of *V. fijiensis* are under positive selection. Meanwhile, the functional annotation shows that distinctly positive selected orthologs in *V. fijiensis* are predominately related to neural signal transduction, immunity, antiapoptotic, and energy metabolism. These results indicate that the mitogenomes and key genes found in transcriptomic analysis are under high-temperature and high-pressure conditions, and which may contribute *V. fijiensis* to have evolved to adapt to the extreme hydrothermal vent environments. The findings shed light on the mitogenome and transcriptome of *V. fijiensis*, which lays a foundation for the in-depth understanding of the adaptation mechanism of sessile invertebrates to the deep-sea environment.

KEYWORDS

barnacle, *Vulcanolepas fijiensis*, deep-sea adaptation, mitogenome, transcriptome

1 Introduction

The general characteristics of the deep-sea environment are high pressure, darkness, and a lack of oxygen. Moreover, the temperature is low and the food source is limited (Danovaro et al., 2014; Lyu et al., 2023). Despite the harsh deep-sea ecosystem, there are still many crustaceans living here, including *Glyptelasma gigas* (Annandale) (Gan et al., 2020b), *Alvinocaris longirostris* (Kikuchi & Ohta) (Hui et al., 2018a; Xin et al., 2021), and *Hirondellea gigas* (Birstein & Vinagradov) (Lan et al., 2017). Additionally, the hereditary characteristics and adaptive evolution of marine organisms may be influenced by these adverse factors. Consequently, a number of reserachers have explored the adaptive evolutionary traits of marine organisms within a specific ecological setting, elucidating the mechanisms by which these organisms adapt to their environment. For instance, the population genetic structure of *Capitulum mitella* (Linnaeus) was explored through single DNA fragments, such as mitochondrial DNA control regions, and a large amount of gene flow was found, indicating that populations living in different regions have significant genetic differentiation due to the differences in their genetic adaptability (Song and Yoon, 2013; Yoon et al., 2013).

In addition, the deep-sea hydrothermal region is the most anoxic and highly toxic marine ecosystem on earth, which plays an important role in mitochondrial division and biological function (Ki et al., 2009). Previous phylogenetic analysis based on fossil and mitochondrial genomes has shown that bathymodiolins (*Bathymodiolus*) gradually evolved characteristics that were adapted to their environment in the process of their origin and evolution (Lorion et al., 2013; Thubaut et al., 2013). However, how bathymodiolin mussels have adapted to deep-sea chemosynthetic environments over the long term, and the genetic bases for these adaptations are still unclear (Zheng et al., 2017). Moreover, there is a lack of molecular data, such as single genes or single proteins, that can be used to deduce the adaptive mechanisms of deep-sea marine organisms. Therefore, it is imperative to conduct an analysis of the crucial mitochondrial functional genes within the immunity metabolic pathway, as this would elucidate the underlying mechanism behind their adaptability to the hydrothermal vent environment.

It is universally acknowledged that the transcriptome can be used to determine the expression of genes at the level of messenger RNA (mRNA) and non-coding RNA transcription and explore the functional genes that are related to environmental adaptation or physiological functions (Wilhelm and Landry, 2009). Consequently, a transcriptomic analysis may also illustrate the adaptive mechanisms of deep-sea organisms in diverse environments. Transcriptome sequencing technology can be used to understand the response of various species to marine ecosystems at the mRNA level, and it has been widely used in researching deep-sea environmental adaptation mechanisms (Zhou et al., 2021; Sun et al., 2022; Yan et al., 2022). For instance, a transcriptomic analysis was conducted on *A. longirostris* from the Iheya North hydrothermal vents and a methane seep in the South China Sea, which found that various genes including *cytochrome P450s* and *Rhodopsin* were related to sulfur metabolism and detoxification, showing their different adaptability between the two extreme conditions (Hui et al., 2018a). Recently, researchers have made significant findings by conducting comparative genomic analysis on deep-sea anemone species. This investigation has led to the identification of multiple genes that exert influence on osmotic metabolism, membrane function, protein translation, and cytoskeleton functions, and which were adapted to the deep-sea environment (Feng et al., 2021). Furthermore, the deep-sea mussel *Gigantidas platifrons* (Hashimoto & Okutani) lived in vent and seep habitats with abundant toxic chemical substances, particularly hydrogen sulfide (H_2S). To adapt to the harsh H_2S-rich environments, its genes control oxidative phosphorylation and the mitochondrial sulfide oxidization pathway, playing important roles in the sulfide tolerance of the mussel (Sun et al., 2022).

Barnacles exhibit a wide widely distribution within the intertidal zone and attaching to marine organisms. Furthermore, certain barnacle have undergone evolutionary adaptations in diverse deep-sea habitats (Sha and Ren, 2015; Chan et al., 2021). Due to their extended attachment to the bottom and confinement to relatively narrow deep zones, deep-sea barnacle adults served as suitable model organisms for conducting research on evolutionary and ecological processes (Gan et al., 2020a). Notably, members of the Scalpellomorpha order have been discovered in hydrothermal vents and cold seeps, suggesting the presence of distinctive adaptive mechanisms enabling their survival in deep-sea chemosynthetic habitats (Gan et al., 2022). However, the difficulty associated with the collection of deep-sea Cirripedia have limited the current research on the barnacle transcriptome to mere transcriptome assembly and the mechanism of barnacle attachment (Al-Aqeel et al., 2016; Ryu et al., 2019; Yan et al., 2020). While studies on other organisms inhabiting extreme deep-sea environments have identified several potential mechanisms, the transcriptome of *Vulcanolepas fijiensis* (Chan) and *Scalpellum stearnsi* (Pilsbry) remains unexplored. Moreover, few studies have investigated the molecular adaptive characteristics that assist with barnacles' survival in deep-sea harsh chemosynthetic habitats. Due to the limited prior investigations concerning the transcriptome of barnacles, particularly with regard to the deep-sea adaptation of *V. fijiensis*, our study attempted to address this research gap.

In this study, we collected deep-sea (*V. fijiensis*) and shallow-water (*S. stearnsi*) individuals at Longqi hydrothermal field on the Southwest Indian Ridge and Guangxi Beibu Gulf, respectively. In order to investigate the adaptability of barnacles to the deep-sea environment, the analysis of positive selection pressure was conducted using the comparative transcriptome of these two individuals, as well as the 13 protein-coding genes (PCGs) of mitogenomes from 11 barnacles, including *V. fijiensis*. This research endeavor aimed to not only provide valuable genomic resources for deep-sea barnacles but also establish a foundation for comprehending their genetic strategies and adaptation mechanisms in the deep-sea habitat.

2 Materials and methods

2.1 Sample collection, DNA and RNA extraction, and sequencing

A variety of manned submarines were used to obtain *V. fijiensis* from a hydrothermal vent Longqi hydrothermal field on the

Southwest Indian Ridge (49°64'E, 37°17'S) at a depth of 2,759 m in the Southwest Indian Ocean. *S. stearnsi* were obtained from the Guangxi Beibu Gulf (109°12'E, 21°04'N), depth of about 300 m. In contrast to deep-sea species, the depth of 300m can be considered relatively shallow. Therefore, we provisionally classified *S. stearnsi* as a shallow species. After collection, they were immediately stored at -80°C.

According to the manufacturer's directions, the TIANamp Marine Animal DNA Kit (TIANGEN Biotech, China) was used to extract DNA from the abdominal muscle. Then, 1% gel electrophoresis and ultraviolet spectroscopy (Eppendorf BioPhotometer D30, Eppendorf, Germany) were used to estimate and quantify the genomic DNA. Then, the DNA was randomly cut into 350 bp fragments, which were repaired at the end and amplified by a polymerase chain reaction to construct the sequencing library. Next, Sanger dideoxy sequencing (*V. fijiensis*) was conducted on an ABI-3730XL (Thermo Fisher Scientific, USA), and high-throughput sequencing (*S. stearnsi*) was conducted on Illumina NovaSeq 6000 platform (TSINGKE Biotechnology Co, Ltd, China).

For each species of barnacle (*V. fijiensis* and *S. stearnsi*), a random selection of three individuals was made, and all RNA was extracted using TRIzol reagent (Invitrogen, USA). The quality of the RNA was assessed through 1% agarose gel electrophoresis. The purity and concentration of the RNA were determined using a NanoPhotometer spectrophotometer (IMPLEN, Germany) and Qubit 2.0 Fluorimeter (Life Technologies, USA), respectively. The integrity of the RNA was evaluated using the RNA Nano 6000 Assay Kit of the Agilent Bioanalyzer 2100 system (Agilent Technologies, USA). The sequencing library was established according to the manufacturer's instructions of the NEBNext Ultra RNA Library Prep Kit (NEB, USA). The mRNA was enriched using poly-T oligo-attached magnetic beads, and an Agilent Bioanalyzer 2100 system (Agilent Technologies) was used to evaluate the synthesis of the complementary DNA (cDNA), the construction of a pair-end library, and the quality of the library. Finally, the two different kinds of species' cDNA libraries were clustered and sequenced using the Illumina HiSeq 2500 platform by NovoGene (Beijing, China).

2.2 Mitogenome assembly, annotation, and analysis

The initial dataset of the mitochondrial genome consisted of 150 base pairs at the paired ends. Reads containing an adapter, reads with a mass score below 20 ($Q< 20$), and duplicated sequences were removed. A reference genome (*Lepas anserifera*) was used to retrieve the reads belonging to the mitochondrial genome for assembly. Then, *de novo* assembly was performed using SPAdes 3.13.0 (Bankevich et al., 2012), and the assembly results were corrected for mutual alignment to confirm the accuracy of the assembled genome sequence. The assembled mitochondrial genomes were subjected to analysis using the online MITOS software (http://mitos.bioinf.unileipzig.de) with default parameters. This software was utilized to predict the PCGs, transfer RNA (tRNA) genes, and ribosomal RNA (*rRNA*) genes. Manual corrections to the genes for the start/stop codons were performed in Sequin 15.10 (http://www.ncbi.nlm.nih.gov/Sequin/index.html) by referencing the mitochondrial genome. On this basis, BLAST (https://blast.ncbi.nlm.nih.gov/Blast.cgi) technology was used to compare the existing research data including the PCGs and *rRNA* to verify and correct the accuracy of the analysis results. The circular mitochondrial genome map was drawn using OGDRAW 1.3.1 (Greiner et al., 2019), and the complete mitogenomes of *V. fijiensis* and *S. stearnsi* have been registered as MZ772032 and OP345466 on GenBank.

The biases for the codon usage of the mitogenome can regulate genes and reflect the evolutionary relationship between different species (Wei et al., 2014). Consequently, the usage of codons was analyzed for the PCGs and *rRNA*. Using the following formula, the inclination related to the nucleotide bases was calculated:

$$\text{adenine (A) and thymine (T) skew} = (A - T) \div (A + T)$$

$$\text{guanine (G) and cytosine (C) skew} = (G - C) \div (G + C)\,.$$

2.3 Transcriptome assembly and annotation

The low-quality reads and reads containing adaptors were removed from the raw reads using the internal software (ng_qc) with custom script of NovoGene, and the transcriptome clean reads were obtained. The *de novo* transcriptome assembly was performed using Trinity v2.5.1, with the minimum k-mer parameter coverage of 2, while default parameters were employed for other sections (Grabherr et al., 2011). The longest transcript of each transcription group was regarded as a unigene for the subsequent analysis. Next, BUSCO v1.22 was used to verify the quality of the assembly that was performed using the arthropoda_odb9 database (Simão et al., 2015). Additionally, all the unigenes were annotated by blasting the common databases, such as the National Center for Biotechnology Information non-redundant protein (Nr), Swiss-Prot, and euKaryotic Ortholog Group using DIAMOND v0.8.22 (Buchfink et al., 2015), and the NCBI nucleotide database using BLAST v2.2.28+ (Altschul et al., 1990). The Kyoto Encyclopedia of Genes and Genomes (KEGG) classification was performed using the KEGG Automatic Annotation Server (Moriya et al., 2007). The protein family (Pfam) alignments were put into practice using HMMER v3.0 (http://hmmer.org/) and were based on the results of Nr and Pfam, and Blast2GO v2.5 was used to classify the Gene Ontology (GO) (Götz et al., 2008). The Nr database was searched for unigenes with BLASTx, and then SOLAR was used to compare the link fragments (Rota-Stabelli et al., 2010), so all the open reading frames (ORF) of the unigenes were obtained and converted into amino acid sequences.

2.4 Identification of the positively selected genes

The target sequences for this analysis consisted of the 13 PCGs from *V. fijiensis* and 10 other barnacle species, aligning using clustalW (codons) in MEGA v7.0. Manual removal of gap and

stop codons was performed to ensure accurate alignment (Kumar et al., 2016). The resulting sequence alignment file was then utilized for the analysis of positive selection. A molecular phylogenetic tree was constructed using the maximum likelihood method in MEGA v7.0 to assess selective pressure. Subsequently, the reconstructed tree was subjected to EasyCodeML in the PAML software (Gao et al., 2019) to identify natural selection characteristics within the 13 PCGs. Among them, the 13 PCGs from *V. fijiensis* were treated as the foreground branch, while PCGs from other barnacle species served as the background branch. Site models were employed to identify the individual sites of PCGs. Changes in the different sites of the 13 PCGs were explored by calculating the ω values ($\omega = K_a/K_s$ or dN/dS). For the positive selection sites ($\omega > 1$), the Bayes Empirical Bayes (BEB) method was used to estimate the Bayesian posterior probabilities (Biswas and Akey, 2006). The likelihood Ratio Test (LRT) was applied to compare the hypothetical models with the corresponding original hypotheses, and the LRT *P*-value was determined using the Chi-square method. The sites of the PCGs with an LRT *P*-value< 0.05 or BEB > 95% were considered to be under evolution and positive selection pressure. The ProtParam program (http://www.expasy.ch/tools/protparam.html) software was utilized to compute the relative molecular weight and isoelectric points of the sequence, and SignalIP 4.1 (http://www.cbs.dtu.dk/services/SignalP/) was employed to predict the signal peptides. Additionally, the SMART program (http://smart.embl-heidelberg.de/) was utilized to predict the conserved functional domains of proteins (Letunic and Bork, 2021). On this basis, we matched the sites to the three-dimensional (3D) conformation of the PCGs to observe their role under positive selection more clearly. The 3D structure of the target proteins was simulated using the SWISS-MODEL (Waterhouse et al., 2018) server, which visualized the positive selection sites in the proteins.

Transcriptome sequence set from the two species (*V. fijiensis* and *S. stearnsi*), internal reference (*Amphibalanus Amphitrite*) and external reference species (*Eurytemora affinis*) were utilized for the analysis of the orthologous genes and nonsynonymous (dN)/synonymous (dS) substitution rates. Subsequently, adaptive evolution was assessed by comparing the ω value (dN/dS). BLAST was employed to pair the orthologs with the best hit probabilities. Following this, sequence alignment was conducted using MUSCLE, and all gaps were eliminated. The ω numerical calculation for each ortholog was performed using PAML v4.48a. Genes with ω values exceeding 1 were considered as positively selected genes (PSGs). The PSGs were further subjected to GO and KEGG enrichment analysis using Omicshare CloudTools (http://www.omicshare.com/tools/), with a significance threshold set at a *q*-value less than 0.05.

3 Results

3.1 Mitogenome organization and composition

The complete mitogenomes of *V. fijiensis* and *S. stearnsi* are 16,960 bp and 15,462 bp in length, respectively. They each contain the general 13 PCGs (*COI*, *COII*, *COIII*, *ATP8*, *ATP6*, *ND1*, *ND2*, *ND3*, *ND4*, *ND4L*, *ND5*, *ND6* and *COB*), 2 *rRNA* genes (16S and 12S *rRNA*), 22 tRNA genes, and a *D*-loop. With the exception of the nicotinamide adenine dinucleotide hydride (NADH) genes (*ND5*, *ND4*, *ND4L*, *ND1*) and eight tRNA genes (*trnF*, *trnQ*, *trnH*, *trnP*, *trnC*, *trnY*, *trnL*, *trnV*), the majority of genes are encoded by the heavy strand (H-strand). Furthermore, apart from a few gene overlaps, the majority of nucleotide gaps are observed between the tRNA. In addition, 16S and 12S are located between $trnL_1$ (TAG), *trnV* (TAC) and *trnW* (TCA) respectively (Figure 1; Table 1).

3.2 Nucleotide composition and bias

The nucleotide compositions (PCGs and *rRNA*) of *V. fijiensis* and *S. stearnsi* are 20.9~39.8% A, 5.3~24.1% C, 32.9~48.3% T, and

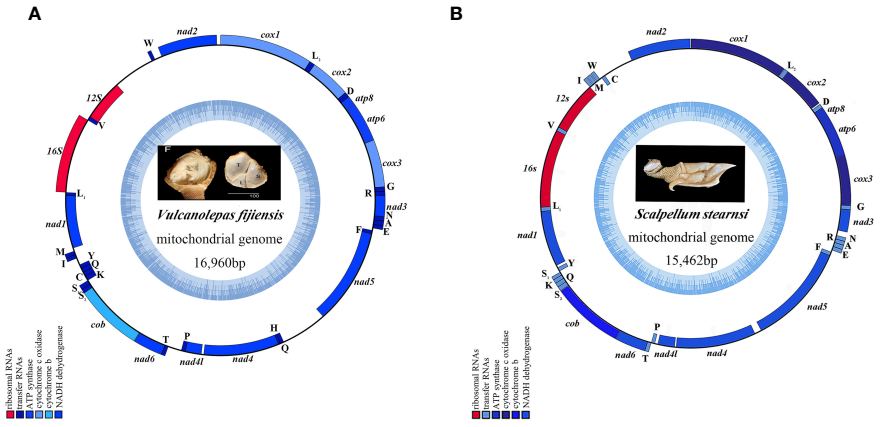

FIGURE 1
The mitochondrial genome map of deep-sea barnacle *Vulcanolepas fijiensis* **(A)** and shallow barnacle *Scalpellum stearnsi* **(B)**. The heavy strand is represented by the outer circle, while the light strand is represented by the inner circle; The tRNA and PCGs are denoted by the blue genes, whereas the 12S *rRNA* and 16S *rRNA* are indicated by the red genes.

10.3389/fmars.2023.1269411

TABLE 1 Summary of the mitogenome features of *Vulcanolepas fijiensis* and *Scalpellum stearnsi*.

Gene	Strand	Size (bp)	Codon		GC percent (%)	Anti-codon	Intergenic nucleotide (bp)
			Inferred start codon	Inferred stop codon			
COI	H	1 549/1 536	ATA/ACG	T-/TAA	34.3-36.1		0/4
trnL$_2$	H	88/66				TAA	0
COII	H	684	ATG	TAA	28.0-33.9		0/20
trnD	H	88/63				GTC	0
ATP8	H	159	ATC/ATA	TAA	23.2-26.5		-7
ATP6	H	666	ATG	TAA	26.9-31.4		-1
COIII	H	789/788	ATG	TAA/TA-	33.9-37.7		0/-1
trnG	H	72/64				TCC	0
trnR	H	69/62				TCG	0
ND3	H	348/354	ATT/ATA	TAA	25.3-33.6		0/84
trnN	H	74/62				GTT	0
trnA	H	76/68				TGC	0
trnE	H	68/64				TTC	37/33
trnF	L	63/64				GAA	0
ND5	L	1 695/1 701	ATT	TAA	28.7-29.6		817/0
trnQ	L	65/68				TTG	0
trnH	L	64				GTG	0
ND4	L	1 329/1 330	ATT/ATG	TAA/T-	28.8-29.6		41/23
ND4L	L	285/282	ATG/ATA	TAA	27.7-29.5		0/47
trnP	L	73/61				TGG	233/0
trnT	H	67/62				TGT	0
ND6	H	492/483	ATT	TAA	23.6-26.2		2/-1
COB	H	1 143/1 140	ATG	TAA	32.2-35.8		0/2
trnS$_2$	H	70				TGA	0
trnS$_1$	H	75/54				TCT	0/19
trnK	L/H	84/61				TTT	0
trnC	L	78/63				GCA	0
trnY	L	66/65				GTA	122/40
trnI	H	68/64				GAT	0/6
trnM	H	66/64				CAT	54/10
ND1	L	924/930	ATA/ATT	TAA	28.6-31.9		0
trnL$_1$	L	58/68				TAG	0
lrRNA	L	1 324/1 301			24.5-27.2		0
trnV	L	67/66				TAC	0
srRNA	L	731/839			26.3-31.6		0
trnW	H	65				TCA	126/36
ND2	H	987/984	ATA/ATT	TAA	25.0-29.8		61/9
D-loop	H	736/507					0

3.1~24.2% G, with an AT content ranging from 62.4% to 76.8% (Supplementary Tables 1, 2). Their majority of the PCGs have a negative AT skew, except for *ND1*, *ND4*, *ND4L*, and *ND5*, which display a positive GC skew (Figure 2).

3.3 Protein-coding genes and codon usage

Except for *COI*, which is encoded by the ACG codon, the start codons of the PCGs predominantly follow canonical sequences (ATT/ATA/ATG). Additionally, within barnacle mitogenomes, three distinct types of stop codons are identified (T-, TA-, and TAA), with TAA being the most prevalent. Moreover, the T- and TA- stop codons only occur in *COI*, *COIII*, and *ND4* of *V. fijiensis* and *S. stearnsi* (Table 1).

The findings show that except for leucine and serine have six to eight codons, the other amino acids of the two examined species have two to four changeable codons (Figure 3). The codon usage analysis demonstrates that the following codon sequences appear with higher frequency: phenylalanine (UUU), isoleucine (AUU), and leucine (UUA). The codons with U or C in the third position occur more frequently than those with A or G. Different from the shallow-sea barnacle, the main amino acids in *V. fijiensis* are asparagine and lysine (Figure 3).

3.4 Transcriptome assembly and annotation

A total of 47,593,764 and 47,752,536 raw reads are generated from *S. stearnsi* and *V. fijiensis*, respectively. BUSCO assessment of assembly quality are showed in Supplementary Figures 1, 2. The complete single-copy and complete duplicated of the two origanisms are over 80%. Through the transcriptome assemblies, there are 98,686 unigenes identified with an N50 length of 916 bp for *S. stearnsi*, and 53,562 unigenes with an N50 length of 1,721 bp for *V. fijiensis*. Among these unigenes, 38,666 (39.18%) and 20,628 (38.51%) are successfully annotated in *S. stearnsi* and *V. fijiensis*, respectively (Table 2).

The Gene Ontology functional cluster analysis indicates that 26,718 and 16,746 unigenes are successfully clustered in the three functional categories of GO (48 functional items). The major biological processes are the cellular, metabolic, and single-organism processes, with *V. fijiensis* lacking the biological phase item and *S. stearnsi* lacking the rhythmic process item. Within the cellular components, the cell and cell part items are identified. The major molecular functions are binding and catalytic activity (Figure 4). In addition, The KEGG functional cluster analysis shows that 6,845 and 12,042 unigenes in *V. fijiensis* and *S. stearnsi* are clustered into five functional groups, respectively, and

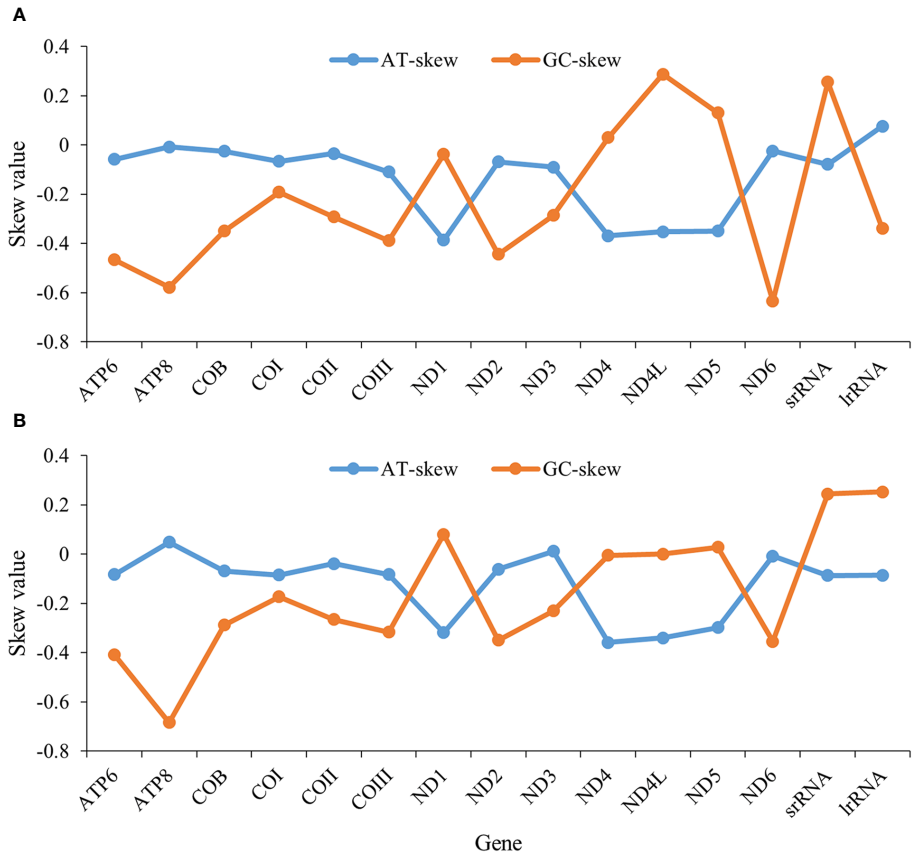

FIGURE 2
AT and GC skews in protein-coding genes of the mitochondrial genomes in deep-sea barnacle *Vulcanolepas fijiensis* **(A)** and shallow barnacle *Scalpellum stearnsi* **(B)**. The horizontal and vertical coordinates represent gene name and skew value, respectively; The blue line represents the AT skew and the orange line represents the GC skew.

10.3389/fmars.2023.1269411

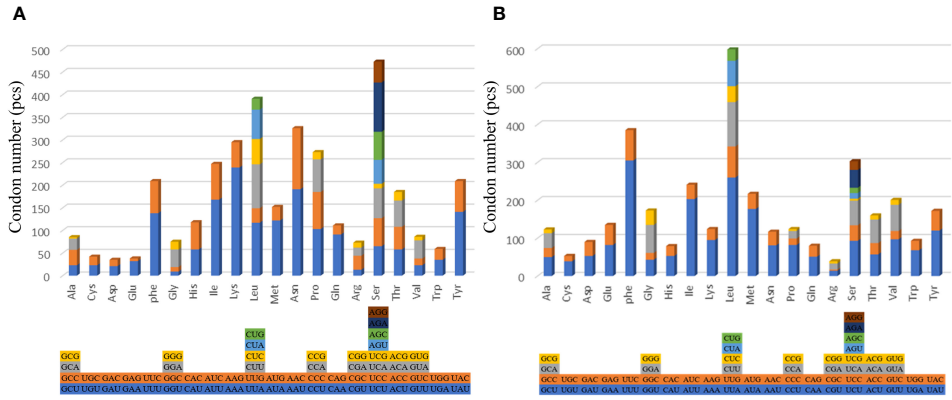

FIGURE 3
The codon usage of the protein-coding genes of the mitochondrial genomes of deep-sea barnacle *Vulcanolepas fijiensis* **(A)** and shallow barnacle *Scalpellum stearnsi* **(B)**. The different colors represent different kinds of codons, and the different columns represent different amino acids.

more genes are annotated in the endocrine system, translation, and signal transduction pathways (Figure 5).

3.5 Positively selected genes analysis

From the complete mitochondrial genome of the 11 barnacle species, namely *V. fijiensis*, *Conchoderma hunteri* (Owen), *Lepas anserifera* Linnaeus, *L. australis* Darwin, *L. anatifera* Linnaeus (Lepadidae), *S. stearnsi*, *Arcoscalpellum epeeum* Chan (Scalpellidae), *Altiverruca navicula* Hoek (Verrucidae), *Capitulum mitella* Linnaeus (Pollicipedidae), *Glyptelasma annandalei* Pilsbry (Poecilasmatidae), and *Ibla cumingi* Darwin (Iblidae) (Table 3), 13 PCGs were extracted for positive selection pressure analysis. The positive selection analysis yielded results indicating that the *COIII* and *ND2* genes ($\omega > 1.0$, $P<0.05$) of deep-sea species experience positive selection pressure. The three-dimensional structure model was utilized to identify and highlight specific sites within the genes that are under positive selection pressure, such as 22I, 29T, and 41E in the *COIII* gene, as well as 73F, 75S, and 76L in the *ND2* gene (Table 4; Figure 6).

Genes that are subjected to positive selection tend to respond to natural selection. We identified 148 pairwise orthologs within *V. fijiensis*, *S. stearnsi* and two reference species in one-to-one correspondence to confirm the PSGs (Supplementary Table 3, Supplementary Figure 3) and performed an adaptive evolutionary analysis on them. The findings reveal the presence of five orthologs, namely chromosome 3 open reading frame 10 (*C3ORF10*), E74-like factor (*ELF*), ubiquitin-like protein ATG12 (*ATG12*), uracil phosphoribosyltransferase (*UPRT*), and small subunit ribosomal protein S21e (*RPS21*), all exhibiting ω values greater than 1.0. Notably, only *RPS21* did not fall below the significance threshold of 0.05 (Table 5; Supplementary Figure 3). These PSGs are mainly enriched in the RIG-I-like receptor signaling, regulation of autophagy, apoptosis-fly, regulation of the actin cytoskeleton, pyrimidine metabolism, foxO signaling, and ribosome pathways (Figure 7; Table 5). It is predicted that the ORFs of the five genes under positive selection pressure are all complete. Except for *C3ORF10*, the amino acid domain positions of the other genes are predicted, there is no signal peptide, and the molecular weight range from 9.21 to 27.23 kDa. Additionally, the isoelectric point is relatively similar, ranging from 6.05 to 9.88 (Supplementary Table 4).

TABLE 2 Transcriptome library basic information of *Scalpellum stearnsi* and *Vulcanolepas fijiensis*.

Class	Item	*Vulcanolepas fijiensis*	*Scalpellum stearnsi*
Assembly	Transcript number (bar)	54,446	99,622
	Unigene number (bar)	53,562	98,686
	Total length of Unigenes (bp)	49,774,143	61,491,550
	N50 length of Unigenes (bp)	1,721	916
	Mean length of Unigenes (bp)	929	623
Annotation	Nr	13,679 (25.53%)	26,304 (26.65%)
	Nt	5,150 (9.61%)	8,036 (8.14%)
	Swiss-Prot	12,019 (22.43%)	19,772 (20.03%)
	KEGG Orthology	6,845 (12.77%)	12,042 (12.2%)
	PFAM	16,685 (31.15%)	26,406 (26.75%)
	GO	16,746 (31.26%)	26,718 (27.07%)
	KOG	7,129 (13.3%)	10,959 (11.1%)
	All Databases	2,422 (4.52%)	2,786 (2.82%)
	At least one database	20,628 (38.51%)	38,666 (39.18%)

4 Discussion

4.1 Mitogenome adaptive evolution

Previous research has identified that certain barnacles exhibit similar arrangement structures within their mitogenomes

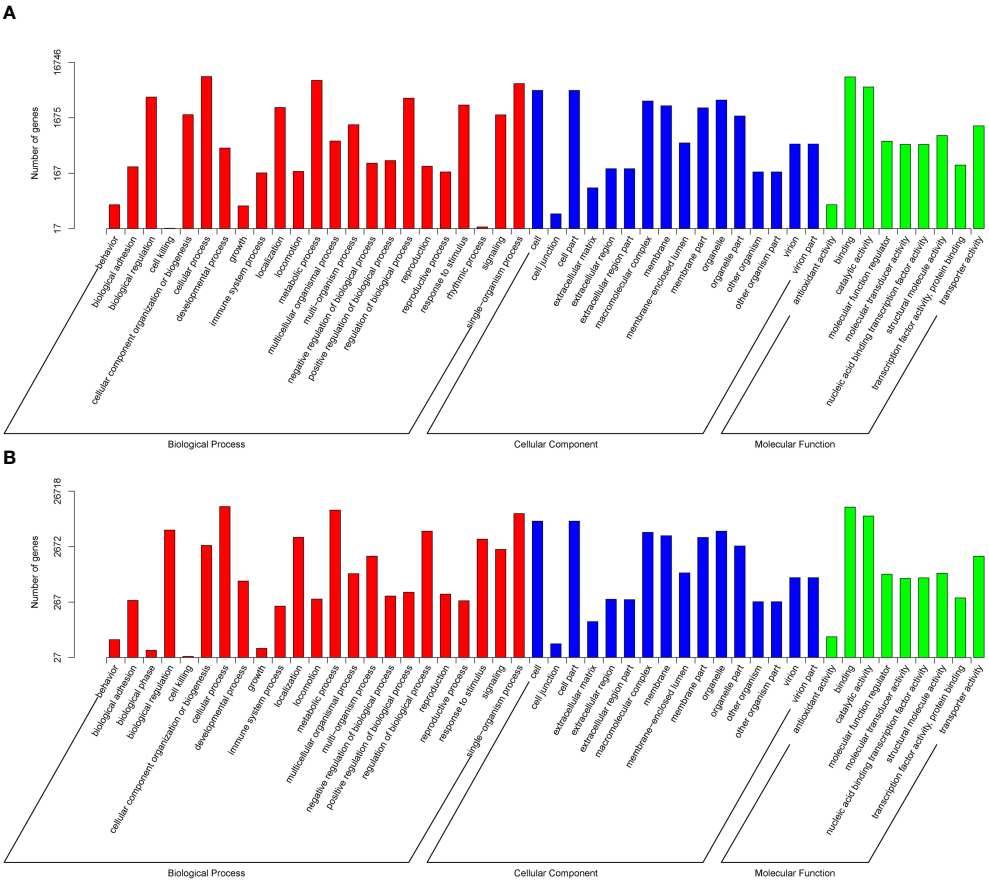

FIGURE 4
Gene Ontology function annotation of the transcriptomes of deep-sea barnacle *Vulcanolepas fijiensis* **(A)** and shallow barnacle *Scalpellum stearnsi* **(B)**. The red terms represent Biological Process, the blue terms represent Cellular Composition, and the green terms represent Molecular Function.

(Shen et al., 2015). We also find similar genetic structures in the mitogenomes of the deep-sea and shallow barnacles. The AT content in the complete mitogenomes of both organisms, exceeded the GC content, aligning with the base composition observed in the majority of invertebrates (Liu et al., 2018; Wang et al., 2021; Sato et al., 2023). More negative AT skews are observed in *ND1*, *ND4*, *ND4L*, and *ND5* genes of the two barnacles (Figure 2). This phenomenon might be attributed to the deep-sea habitat of these organisms, where DNA replication and transcription processes are subject to the mutations and the natural selection resulting in a bias towards specific nucleotides (Sahyoun et al., 2014; Yu et al., 2019). It is speculated that the different genetic structures of these four genes might be closely related to the pressure of natural selection in the extreme habitats. However, how nucleotide bias affects the initiation and orientation of gene replication and what selective pressures induced nucleotide skews need further study. Furthermore, the amino acid usage patterns observed in *V. fijiensis* are similar to those of the shallow barnacle *S. stearnsi* (Figure 3), which provides more evidence for the barnacle nucleotide composition and gene skew results. Generally, more than 95% of energy comes from the oxidative phosphorylation of mitochondria (Auger et al., 2021). In the abyssal zone, the dark and absence of autotrophic primary producers pose constraints on the availability of sustenance (Gattuso et al., 2006). The observed nucleotide compositional biases between *V. fijiensis* and *S. stearnsi* indicated that, in their mitogenomes, comparable alterations occurred during the evolutionary progression which might be a means of adapting to the extreme conditions and nutritional scarcity of the deep-sea environment.

Mitochondria serve as a vital pathway for aerobic respiration within cells. To cope with the extreme environment, selection pressure would have been put on the mitogenome, and non-synonymous mutations are regarded as an adaptive substitution to meet the needs of a new environment (Srivastava et al., 2020). The results of our study indicate that the mitogenomes in *V. fijiensis* experienced significant selective pressure, particularly the *COIII* and *ND2* genes, which have specific functional protein sites (Table 4; Figure 6). There is a prevalent belief that functional proteins contain positive selection sites, which serve as a foundation for adaptive responses to alterations in the environment (Rausher and Huang, 2016). *COIII* is one of the core members of cytochrome *C* oxidase, a key rate-limiting enzyme at the end of the mitochondrial respiratory chain, which produces ATP and changes oxygen into water for cell metabolism (Timón-Gómez et al., 2018). At the level of mitochondrial transcription and translation, during the respiratory chain embedding in the inner mitochondria, the

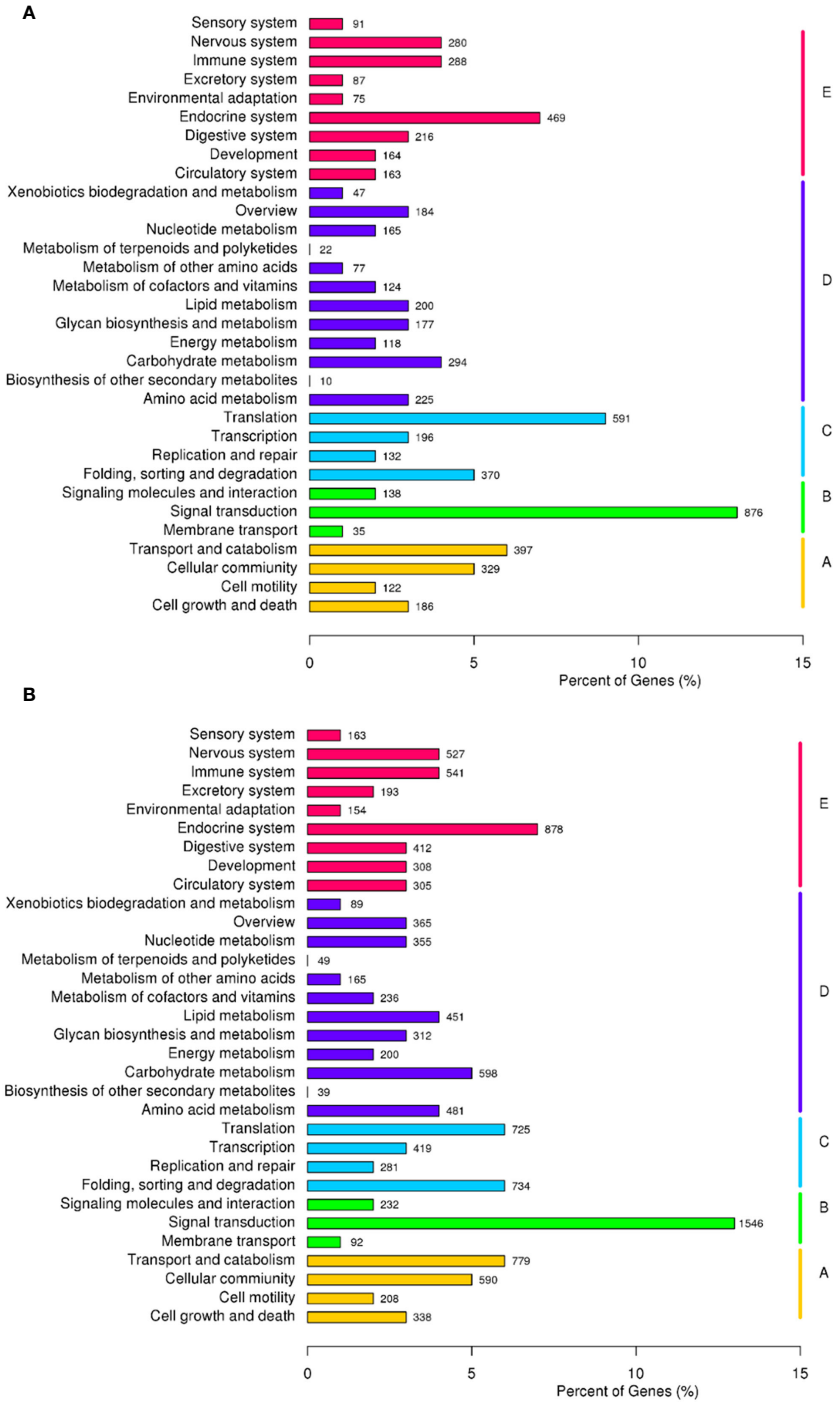

FIGURE 5
Classification of the Kyoto Encyclopedia of Genes and Genomes metabolic pathway of the transcriptomes of deep-sea barnacle *Vulcanolepas fijiensis* **(A)** and shallow barnacle *Scalpellum stearnsi* **(B)**. Vertical lines represent five main pathways: red terms denote cellular processes, purple terms denote environmental information processing, blue terms denote genetic information processing, green terms denote metabolism, and yellow terms denote organismal systems.

respiratory supercomplex factor protein family acts in response to biological hypoxia by binding to *COIII* to adapt to environmental and metabolic changes (Lobo-Jarne and Ugalde, 2018). Through bioinformatics analysis, several adaptive residues potentially presented in *COIII* and *ND2* of alvinocaridid shrimp (Alvinocarididae) inhabiting the deep-sea hydrothermal vent environment also have been identified by researchers. These proteins played an important role in regulating mitogenome intracellular energy metabolism and contributed to the adaptation of organisms to the hydrothermal vent environment (Hui et al.,

TABLE 3 Collection and mitogenome information of the specimens that were used for the positive selection analysis.

Species	Mitochondrial genome size	GenBank accession numbers
Vulcanolepas fijiensis	16,960 bp	MZ772032
Conchoderma hunteri	15,202 bp	OL606642
Scalpellum stearnsi	15,462 bp	OP345466
Lepas anserifera	15,653 bp	OP377772
Lepas australis	15,502 bp	NC025295
Lepas anatifera	15,708 bp	NC062431
Capitulum mitella	14,916 bp	AB167462
Arcoscalpellum epeeum	15,593 bp	MH791047
Altiverruca navicula	15,976 bp	NC037244
Glyptelasma annandalei	16,107 bp	NC043898
Ibla cumingi	15,053 bp	NC066682

2018b). Consequently, we speculate that the PCGs help *V. fijiensis* to resist multiple pressures when adapting to the deep-sea environment.

The NADH dehydrogenases are the largest enzyme complex in the mitochondrial electron transport chain; thus, mutations in these subunits may disturb the efficiency of the electron transport process (Da Fonseca et al., 2008). The NADH dehydrogenase genes of deep-sea anemones exhibited novel genetic structures, which were evidence of adaptation to the deep-sea environment (Zhang et al., 2017). Likewise, the hydrothermal vent environment may potentially exert potential selection pressure on NADH dehydrogenase genes from mitogenomes in *V. fijiensis*. This pressure may influence the modulation of mitochondrial complexes and electron transport efficiency and hence, adapting to cold and hypoxic conditions (Luo et al., 2012). Given the crucial role of mitochondria in aerobic respiration and their indispensability for metabolism and energy production, they likely aid the deep-water barnacle in surmounting the constraints imposed by hypoxia, cold and food availability. Additionally, hydrothermal vents are also associated with hydrogen sulfide (H_2S), and the primary cytotoxic effect of H_2S is to interrupt the mitochondrial respiratory chain by directly inhibiting cytochrome *C* oxidase (Cooper and Brown, 2008). Therefore, we infer that the mitogenomes of *V. fijiensis* are subjected to multiple selection pressures which led to adaptation to the hydrothermal vent environment under extreme deep-sea conditions.

TABLE 4 Results of the selective pressure acting on the protein-coding genes of *Vulcanolepas fijiensis*.

Gene	Model compared	*P*-value	Positive sites
	M1 vs M2/M7 vs M8		
ATP6	$\omega = 1.000/\omega = 1.000$	1.000/0.999	
ATP8	$\omega = 1.000/\omega = 1.000$	0.005/0.999	
COI	$\omega = 26.392/\omega = 1.000$	1.000/0.042	
COII	$\omega = 117.282/\omega = 1.000$	0.999/0.000	
COIII	$\omega = 3.804/\omega = 3.626$	0.000/0.000	22I, 29T etc
COB	$\omega = 34.321/\omega = 1.000$	1.000/0.000	
ND1	$\omega = 1.000/\omega = 1.000$	1.000/0.000	
ND2	$\omega = 26.634/\omega = 1.368$	0.001/0.000	73F, 75S etc
ND3	$\omega = 38.788/\omega = 1.000$	0.999/0.019	
ND4	$\omega = 1.000/\omega = 1.000$	1.000/0.191	
ND4l	$\omega = 1.000/\omega = 1.000$	0.999/0.923	
ND5	$\omega = 976.933/\omega = 15.264$	0.999/0.597	
ND6	$\omega = 40.205/\omega = 1.000$	0.00/0.999	

4.2 Key genes implicated in deep-sea adaptation

Since they cannot swim in the ocean, barnacles are constrained to inhabit a comparatively restricted narrow region, rendering the process of acclimating to the deep-sea milieu arduous. The Southwest Indian Ridge (SWIR) is a typical ultraslow-spreading oceanic ridge, and the Longqi hydrothermal field is the first confirmed active field on the SWIR. Due to the general lack of deep-sea sediments in this hydrothermal zone, which can provide good channels for hydrothermal circulation and spillage, there are a large number of sulfides (Liang et al., 2023). The extreme environment impacts on population vicariance and dispersal, both significant biological processes. However, few researches have focused on the biodiversity of this region (Zhou et al., 2018). Therefore, our research endeavors to fill this gap by examining the effects of *V. fijiensis* and *S. stearnsi* in the marine habitat, thereby enhancing our understanding of the adaptations in the harsh deep-sea environment.

ATG12, a core autophagy protein. The interaction between *ATG12* and its active complex can form autophagosome. Autophagy is an evolutionarily conserved catabolic process that generally promotes cell survival by eliminating intracellular pathogens and removing damaged organelles, playing a pivotal role in cellular homeostasis and adaptation to adverse environments (Chen et al., 2014). During autophagy, *ATG12* binds the E2 ubiquitin conjugating enzyme to form sulfolipid intermediate, which further mediate the binding of phosphatidylethanolamine to LC3 to promote autophagy formation (Yuan et al., 2022). Although the regulation of this process remains incompletely understood, it has been found to induce the formation of the autophagosome membrane and type I interferons (*IFNs*). The process have been shown to play a crucial role in the antiviral immunity of *Larimichthys crocea* (Richardson) (Wei et al., 2021), *Epinephelus coioides* (Hamilton) (Li et al., 2019), and

10.3389/fmars.2023.1269411

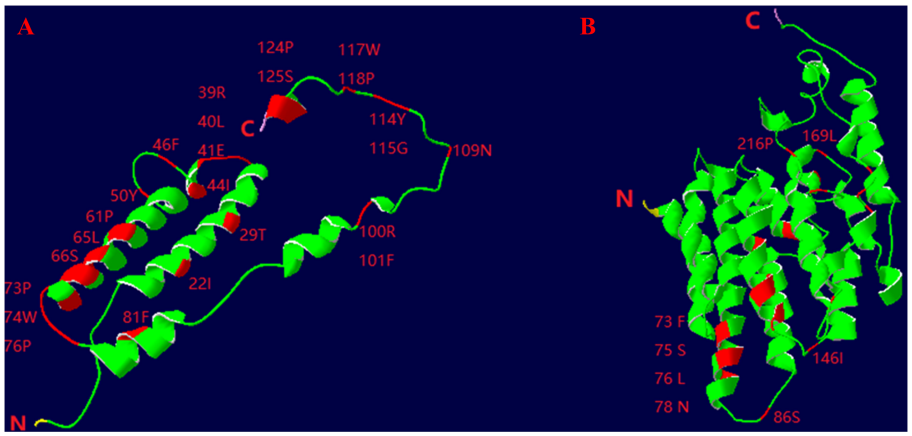

FIGURE 6
Three-dimensional structural models of the *COIII* **(A)** and *ND2* **(B)** genes of deep-sea barnacle *Vulcanolepas fijiensis*. The red represents positive selection site; N represents amino terminus and **(C)** represents carboxy terminus.

TABLE 5 Genes that were subject to positive selection pressure in *Vulcanolepas fijiensis* and *Scalpellum stearnsi*.

Gene	Term	orthologs	dN/dS value	*q*-value
chromosome 3 open reading frame 10, *C3ORF10*	Regulation of actin cytoskeleton	OG14862	3.68	0.04
E74-like factor, *ELF*	Apoptosis - fly	OG15174	11.42	0.04
ubiquitin-like protein ATG12, *ATG12*	RIG-I-like receptor signaling pathway	OG15260	4.30	0.01
ubiquitin-like protein ATG12, *ATG12*	Regulation of autophagy	OG15260	4.30	0.01
ubiquitin-like protein ATG12, *ATG12*	FoxO signaling pathway	OG15260	4.30	0.04
uracil phosphoribosyltransferase, *UPRT*	Pyrimidine metabolism	OG15292	7.84	0.04
small subunit ribosomal protein S21e, *RPS21*	Ribosome	OG14951	20.76	0.12

Ctenopharyngodon idella (Valenciennes in Cuvier and Valenciennes) (Chu et al., 2019), shedding light on the potential involvement of *ATG12* in antiviral immunity by stimulating both autophagy and type I interferon response. Consequently, it is hypothesized that *ATG12* may eliminate intracellular pathogens and damaged celles within *V. fijiensis* by regulating autophagy homeostasis, which have contributed to its adaptation of harsh deep-sea environments. Furthermore, previous studies have demonstrated the involvement of *ATG12* in various cell biological processes such as viability, apoptosis, and autophagy (Wei et al., 2019). Meanwhile, *ATG12* has been found to directly modulate the mitochondrial apoptotic pathway by binding and inactivating prosurvival Bcl-2 family members (Rubinstein et al., 2011). In contrast to barnacles residing in shallow waters, the survival of *V. fijiensis* exposed to diverse toxic substances, including H_2S. This exposure may have potentially facilitated the evolution of more effective immune responses and antiapoptotic metabolism (Cooper and Brown, 2008; Liang et al., 2023).

In Addition, the *ELF* (OG15174) and *UPRT* (OG15292) genes are also positively selected from the enriched pathways of apoptosis-fly and pyrimidine metabolism in *V. fijiensis*, and they are both involved in adaptive immune responses. *ELF*, a pleiotropic transcription factor that modulates disease susceptibility and mediates several biotic and abiotic stress processes, playing a significant role in the host innate immune defense system (Suico et al., 2017). pH, temperature, and salinity can affect the immune response of crustaceans. *ELF* was involved in regulatory processes in organisms through synergistic or retrograde interactions, maintaining osmotic pressure homeostasis (Zhang et al., 2019). Previous researches has demonstrated that *ELF* was significantly expressed in the hepatopancreas and gill tissue of *Penaeus monodon* Fabricius under salt stress, showing that *ELF* was involved in the immune stress process of organisms by regulating immune responses and the development of immune-related cells (Si et al., 2022). Simultaneously, *UPRT* maintains the immunocompetent and regulates the sensitivity of organisms to harmful cells (Koyama et al., 2000; Hasegawa et al., 2013). *UPRT* is a pyrimidine salvage enzyme. It can convert 5-flurouracil to a toxic compound, which kills the deleterious cells but subsequent conversion to other metabolites enhances its anti-apoptotic effect, by irreversibly inhibiting thymidylate synthase, DNA synthesis and the processing of rRNA and mRNA (Gopinath and Ghosh, 2008).

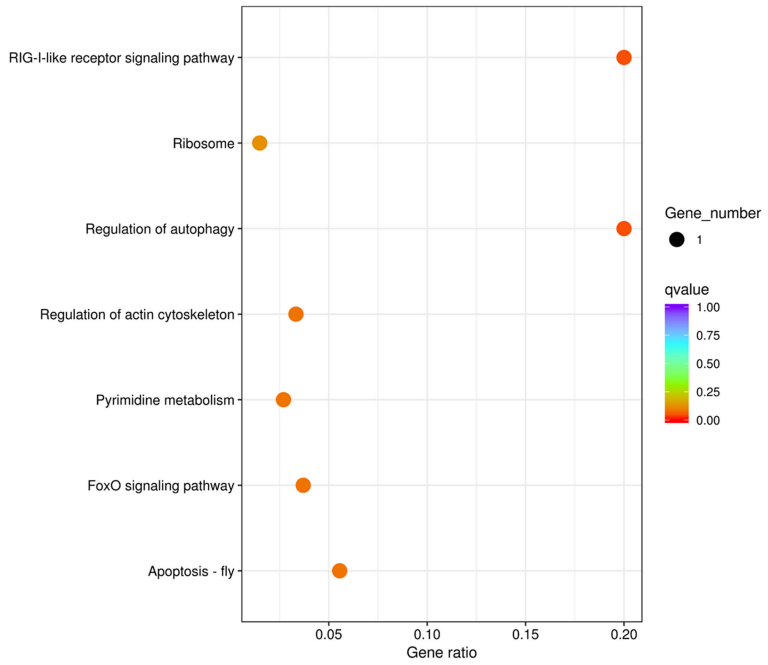

FIGURE 7
Enrichment of the Kyoto Encyclopedia of Genes and Genomes metabolic pathway of the positive selection genes in deep-sea barnacle *Vulcanolepas fijiensis* compared with shallow barnacle *Scalpellum stearnsi*. The circle size represents the number of genes, and the color from cool to warm represents the smaller *q* value.

Thus, it is plausible that these PSGs can potentially contribute to maintaining the immune system of *V. fijiensis*, enabling it to withstand the adverse conditions of the deep sea, including low temperatures and toxic substances. Furthermore, high hydrostatic pressure and low temperatures have caused the inhibition of ligand binding and ion channel function which in turn affected signal transduction (Shinozaki and Yamaguchi-Shinozaki, 2000; Siebenaller, 2000). *C3ORF10* has been proposed to regulate actin dynamics, and its expression played a role in regulating actin dynamics during the process of neurite outgrowth (Stradal and Scita, 2006). *C3ORF10* is a member of the SCAR/WAVE complex, which is the effector of Rac1 to regulate actin dynamics, regulating Arp2/3-dependent actin polymerization and the number of axonal collaterals and dendrites (Wang et al., 2013). Consequently, the genes that have undergone positive selection and involved energy utilization, immune response, and signal transduction metabolism, might enhance the ability of *V. fijiensis* to effectively employ various diverse adaptive strategies within the extreme conditions of the deep-sea environment. *V. fijiensis* also exhibits enrichment of several significant pathways involving genes subject to positive selection, including the apoptosis-fly, regulation of actin cytoskeleton, pyrimidine metabolism, and ribosome pathways. Functionally, the ribosome pathway (K02971) influences almost every aspect of cell and organismal biology including maintaining cell homeostasis in response to changing environmental conditions and acute stress (Ni and Buszczak, 2023). Moreover, impairment of translation can result in the activation of the ribotoxic stress response, implying that ribosomes serve as a signal for the metabolic regulation of stress response (Snieckute et al., 2022), and the inhibition of ribosomal activity hinders the progression of the cell cycle, thereby regulating the adaptive stress response (Stoneley et al., 2022). Consequently, the presence of genes enriched in the ribosomal pathway indicates that the organisms have experienced environmental stress in their habitat.

5 Conclusions

This study is the first to sequence the transcriptome of a deep-sea barnacle *V. fijiensis* and compared it with a shallow-water related species. The presence of positive selection in the mitogenome of *V. fijiensis* suggested that this species probably evolved efficient adaption to cope with the challenges posed by the extreme deep-sea conditions, including limited oxygen and food availability, as well as a high concentration of H_2S in the hydrothermal vent environment. Moreover, the identified PSGs from the enriched KEGG pathways are involved in crucial biological processes such as neural signal transduction, immunity, and antiapoptotic metabolism. Nevertheless, it should be noted that the findings presented in this study are preliminary, and additional research is needed to fully understand the evolutionary and adaptive processes of PSGs in the hydrothermal vent environment. Nonetheless, this study provided valuable genomic resources and insighted into the mechanisms of *V. fijiensis* and *S. stearnsi*, serving as a foundation for further investigations into the evolution and adaptation of invertebrates within deep-sea ecosystems.

Data availability statement

The original contributions presented in the study are publicly available. This data can be found here: https://www.ncbi.nlm.nih.gov/, BioProject: PRJNA935972.

Author contributions

NM: Data curation, Formal analysis, Methodology, Software, Writing – original draft. WS: Data curation, Formal analysis, Methodology, Software, Writing – original draft. YC: Conceptualization, Funding acquisition, Project administration, Resources, Writing – review & editing. XK: Methodology, Project administration, Writing – review & editing. NJ: Methodology, Project administration, Writing – review & editing. XS: Conceptualization, Funding acquisition, Project administration, Resources, Writing – review & editing.

Funding

The author(s) declare financial support was received for the research, authorship, and/or publication of this article. This work was supported by the Natural Science Foundation of China (#42376139), the Jiangsu Provincial Basic Research Program (Natural Science Foundation) Distinguished Youth Fund Project (BK20190048), Postgraduate Research & Practice Innovation Program of Jiangsu Ocean University (KYCX2023-69), Jiangsu Agriculture Science and Technology Innovation Fund (JASTIF) [CX (22) 2032], and the Project Funded by the Priority Academic Program Development of Jiangsu Higher Education Institutions (PAPD).

Conflict of interest

The authors declare that the research was conducted in the absence of any commercial or financial relationships that could be construed as a potential conflict of interest.

Publisher's note

All claims expressed in this article are solely those of the authors and do not necessarily represent those of their affiliated organizations, or those of the publisher, the editors and the reviewers. Any product that may be evaluated in this article, or claim that may be made by its manufacturer, is not guaranteed or endorsed by the publisher.

Supplementary material

The Supplementary Material for this article can be found online at: https://www.frontiersin.org/articles/10.3389/fmars.2023.1269411/full#supplementary-material

References

Al-Aqeel, S., Ryu, T., Zhang, H. M., Chandramouli, K. H., and Ravasi, T. (2016). Transcriptome and proteome studies reveal candidate attachment genes during the development of the barnacle *Amphibalanus amphitrite*. *Front. Mar. Sci.* 3. doi: 10.3389/fmars.2016.00171

Altschul, S. F., Gish, W., Miller, W., Myers, E. W., and Lipman, D. J. (1990). Basic local alignment search tool. *J. Mol. Biol.* 215, 403–410. doi: 10.1016/S0022-2836(05)80360-2

Auger, C., Vinaik, R., Appanna, V. D., and Jeschke, M. G. (2021). Beyond mitochondria: Alternative energy-producing pathways from all strata of life. *Metabolism* 118. doi: 10.3389/fmars.2016.00171

Bankevich, A., Nurk, S., Antipov, D., Gurevich, A. A., Dvorkin, M., Kulikov, A. S., et al. (2012). SPAdes: a new genome assembly algorithm and its applications to single-cell sequencing. *J. Comput. Biol.* 19, 455–477. doi: 10.1089/cmb.2012.0021

Biswas, S., and Akey, J. M. (2006). Genomic insights into positive selection. *Trends. Genet.* 22, 437–446. doi: 10.1016/j.tig.2006.06.005

Buchfink, B., Xie, C., and Huson, D. H. (2015). Fast and sensitive protein alignment using DIAMOND. *Nat. Methods* 12, 59–60. doi: 10.1038/nmeth.3176

Chan, B. K., Dreyer, N., Gale, A. S., Glenner, H., Ewers-Saucedo, C., Pérez-Losada, M., et al. (2021). The evolutionary diversity of barnacles, with an updated classification of fossil and living forms. *Zool. J. Linn Soc* 193, 789–846. doi: 10.1093/zoolinnean/zlaa160

Chen, Z. H., Cao, J. F., Zhou, J. S., Liu, H., Che, L. Q., Mizumura, K., et al. (2014). Interaction of caveolin-1 with ATG12-ATG5 system suppresses autophagy in lung epithelial cells. *Am. J. Physiol. Lung Cell Mol. Physiol.* 306, L1016–L1025. doi: 10.1152/ajplung.00268.2013

Chu, P. F., He, L. B., Yang, C., Zeng, W. C., Huang, R., Liao, L. J., et al. (2019). Grass carp ATG5 and ATG12 promote autophagy but down-regulate the transcriptional expression levels of IFN-I signaling pathway. *Fish. Shellfish. Immunol.* 92, 600–611. doi: 10.1016/j.fsi.2019.06.014

Cooper, C. E., and Brown, G. C. (2008). The inhibition of mitochondrial cytochrome oxidase by the gases carbon monoxide, nitric oxide, hydrogen cyanide and hydrogen sulfide: chemical mechanism and physiological significance. *J. Bioenerg. Biomembr.* 40, 533–539. doi: 10.1007/s10863-008-9166-6

Da Fonseca, R. R., Johnson, W. E., O'brien, S. J., Ramos, M. J., and Antunes, A. (2008). The adaptive evolution of the mammalian mitochondrial genome. *BMC. Genomics* 9, 119. doi: 10.1186/1471-2164-9-119

Danovaro, R., Snelgrove, P. V., and Tyler, P. (2014). Challenging the paradigms of deep-sea ecology. *Trends. Ecol. Evol.* 29, 465–475. doi: 10.1016/j.tree.2014.06.002

Feng, C. G., Liu, R. Y., Xu, W. J., Zhou, Y., Zhu, C. L., Liu, J., et al. (2021). The genome of a new anemone species (Actiniaria: Hormathiidae) provides insights into deep-sea adaptation. *Deep. Sea. Res. 1. Oceanogr. Res. Pap.* 170, 103492. doi: 10.1016/j.dsr.2021.103492

Gan, Z. B., Jones, D. S., Liu, X. M., Sui, J. X., Dong, D., and Li, X. Z. (2022). Phylogeny and adaptative evolution to chemosynthetic habitat in barnacle (Cirripedia: Thoracica) revealed by mitogenomes. *Front. Mar. Sci.* 9. doi: 10.3389/fmars.2022.964114

Gan, Z. B., Xu, P., Li, X. Z., and Wang, C. S. (2020a). Integrative taxonomy reveals two new species of stalked barnacle (Cirripedia, thoracica) from seamounts of the western pacific with a review of barnacles distributed in seamounts worldwide. *Front. Mar. Sci.* 7. doi: 10.3389/fmars.2020.582225

Gan, Z. B., Yuan, J. B., Liu, X. M., Dong, D., Li, F. H., and Li, X. Z. (2020b). Comparative transcriptomic analysis of deep-and shallow-water barnacle species (Cirripedia, Poecilasmatidae) provides insights into deep-sea adaptation of sessile crustaceans. *BMC. Genomics* 21, 1–13. doi: 10.1186/s12864-020-6642-9

Gao, F. L., Chen, C. J., Arab, D. A., Du, Z. G., He, Y. H., and Ho, S. Y. (2019). EasyCodeML: A visual tool for analysis of selection using CodeML. *Ecol. Evol.* 9, 3891–3898. doi: 10.1002/ece3.5015

Gattuso, J. P., Gentili, B., Duarte, C. M., Kleypas, J., Middelburg, J. J., and Antoine, D. (2006). Light availability in the coastal ocean: impact on the distribution of benthic photosynthetic organisms and their contribution to primary production. *Biogeosciences* 3, 489–513. doi: 10.5194/bg-3-489-2006

Gopinath, P., and Ghosh, S. S. (2008). Implication of functional activity for determining therapeutic efficacy of suicide genes *in vitro*. *Biotechnol. Lett.* 30, 1913–1921. doi: 10.1007/s10529-008-9787-1

Götz, S., García-Gómez, J. M., Terol, J., Williams, T. D., Nagaraj, S. H., Nueda, M. J., et al. (2008). High-throughput functional annotation and data mining with the Blast2GO suite. *Nucleic. Acids Res.* 36, 3420–3435. doi: 10.1093/nar/gkn176

Grabherr, M. G., Haas, B. J., Yassour, M., Levin, J. Z., Thompson, D. A., Amit, I., et al. (2011). Full-length transcriptome assembly from RNA-Seq data without a reference genome. *Nat. Biotechnol.* 29, 644–652. doi: 10.1038/nbt.1883

Greiner, S., Lehwark, P., and Bock, R. (2019). OrganellarGenomeDRAW (OGDRAW) version 1.3. 1: expanded toolkit for the graphical visualization of organellar genomes. *Nucleic. Acids Res.* 47, W59–W64. doi: 10.1101/545509

Hasegawa, N., Abei, M., Yokoyama, K. K., Fukuda, K., Seo, E., Kawashima, R., et al. (2013). Cyclophosphamide enhances antitumor efficacy of oncolytic adenovirus expressing uracil phosphoribosyltransferase (UPRT) in immunocompetent Syrian hamsters. *Int. J. Cancer.* 133, 1479–1488. doi: 10.1002/ijc.28132

Hui, M., Cheng, J., and Sha, Z. L. (2018a). Adaptation to the deep-sea hydrothermal vents and cold seeps: insights from the transcriptomes of *Alvinocaris longirostris* in both environments. *Deep. Sea. Res. 1. Oceanogr. Res. Pap.* 135, 23–33. doi: 10.1016/j.dsr.2018.03.014

Hui, M., Wang, M. X., and Sha, Z. L. (2018b). The complete mitochondrial genome of the alvinocaridid shrimp *Shinkaicaris leurokolos* (Decapoda, Caridea): Insight into the mitochondrial genetic basis of deep-sea hydrothermal vent adaptation in the shrimp. *Comp. Biochem. Physiol. Part. D. Genomics Proteomics.* 25, 42–52. doi: 10.1016/j.cbd.2017.11.002

Ki, J. S., Dahms, H. U., Hwang, J. S., and Lee, J. S. (2009). The complete mitogenome of the hydrothermal vent crab *Xenograpsus testudinatus* (Decapoda, Brachyura) and comparison with brachyuran crabs. *Comp. Biochem. Physiol. Part. D. Genomics Proteomics.* 4, 290–299. doi: 10.1016/j.cbd.2009.07.002

Koyama, F., Sawada, H., Fujii, H., Hamada, H., Hirao, T., Ueno, M., et al. (2000). Adenoviral-mediated transfer of Escherichia coli uracil phosphoribosyltransferase (UPRT) gene to modulate the sensitivity of the human colon cancer cells to 5-fluorouracil. *Eur. J. Cancer.* 36, 2403–2410. doi: 10.1016/S0959-8049(00)00338-5

Kumar, S., Stecher, G., and Tamura, K. (2016). MEGA7: molecular evolutionary genetics analysis version 7.0 for bigger datasets. *Mol. Biol. Evol.* 33, 1870–1874. doi: 10.1093/molbev/msw054

Lan, Y., Sun, J., Tian, R., Bartlett, D. H., Li, R. S., Wong, Y. H., et al. (2017). Molecular adaptation in the world's deepest-living animal: Insights from transcriptome sequencing of the hadal amphipod *Hirondellea gigas*. *Mol. Ecol.* 26, 3732–3743. doi: 10.1111/mec.14149

Letunic, L., and Bork, P. (2021). Interactive Tree Of Life (iTOL) v5: an online tool for phylogenetic tree display and annotation. *Nucleic. Acids Res.* 49, W293–W296. doi: 10.1093/nar/gkab301

Li, C., Yu, Y. P., Zhang, X., Wei, J. G., and Qin, Q. W. (2019). Grouper Atg12 negatively regulates the antiviral immune response against Singapore grouper iridovirus (SGIV) infection. *Fish. Shellfish. Immunol.* 93, 702–710. doi: 10.1016/j.fsi.2019.08.037

Liang, J., Tao, C. H., Zheng, Y., Zhang, G. Y., Su, C., Yang, W. F., et al. (2023). Geology context, vent morphology, and sulfide paragenesis of the Longqi-1 modern seafloor hydrothermal system on the ultraslow-spreading Southwest Indian ridge. *Deep. Sea. Res. 1. Oceanogr. Res. Pap.* 194, 103962. doi: 10.1016/j.dsr.2023.103962

Liu, J., Liu, H. L., and Zhang, H. B. (2018). Phylogeny and evolutionary radiation of the marine mussels (Bivalvia: Mytilidae) based on mitochondrial and nuclear genes. *Mol. Phylogenet. Evol.* 126, 233–240. doi: 10.1016/j.ympev.2018.04.019

Lobo-Jarne, T., and Ugalde, C. (2018). Respiratory chain supercomplexes: structures, function and biogenesis. *Semin. Cell. Dev. Biol.* 76, 179–190. doi: 10.1016/j.semcdb.2017.07.021

Lorion, J., Kiel, S., Faure, B., Kawato, M., Ho, S. Y., Marshall, B., et al. (2013). Adaptive radiation of chemosymbiotic deep-sea mussels. *Proc. R. Soc Lond. B. Biol. Sci.* 280, 20131243. doi: 10.1098/rspb.2013.1243

Luo, Y., Chen, Y., Liu, F., and Gao, Y. (2012). Mitochondrial genome of Tibetan wild ass (*Equus kiang*) reveals substitutions in NADH which may reflect evolutionary adaptation to cold and hypoxic conditions. *Asia. Life. Sci.* 21, 1–11.

Lyu, L., Fang, K., Zhu, Z., Li, J., Chen, Y., Wang, L., et al. (2023). Bioaccumulation of emerging persistent organic pollutants in the deep-sea cold seep ecosystems: Evidence from chlorinated paraffin. *J. Hazard. Mater.* 445, 130472. doi: 10.1016/j.jhazmat.2022.130472

Moriya, Y., Itoh, M., Okuda, S., Yoshizawa, A. C., and Kanehisa, M. (2007). KAAS: an automatic genome annotation and pathway reconstruction server. *Nucleic. Acids Res.* 35, W182–W185. doi: 10.1093/nar/gkm321

Ni, C., and Buszczak, M. (2023). The homeostatic regulation of ribosome biogenesis. *Cell. Dev. Biol.* 136, 13–26. doi: 10.1016/j.semcdb.2022.03.043

Rausher, M. D., and Huang, J. (2016). Prolonged adaptive evolution of a defensive gene in the solanaceae. *Mol. Biol. Evol.* 33, 143–151. doi: 10.1093/molbev/msv205

Rota-Stabelli, O., Kayal, E., Gleeson, D., Daub, J., Boore, J. L., Telford, M. J., et al. (2010). Ecdysozoan mitogenomics: evidence for a common origin of the legged invertebrates, the Panarthropoda. *Genome. Biol. Evol.* 2, 425–440. doi: 10.1093/gbe/evq030

Rubinstein, A. D., Eisenstein, M., Ber, Y., Bialik, S., and Kimchi, A. (2011). The autophagy protein Atg12 associates with antiapoptotic Bcl-2 family members to promote mitochondrial apoptosis. *Mol. Cell.* 44, 698–709. doi: 10.1016/j.molcel.2011.10.014

Ryu, T., Woo, S., and Lee, N. (2019). The first reference transcriptome assembly of the stalked barnacle, *Neolepas marisindica*, from the Onnuri Vent Field on the Central Indian Ridge. *Mar. Genomics* 48, 100679. doi: 10.1016/j.margen.2019.04.004

Sahyoun, A. H., Bernt, M., Stadler, P. F., and Tout, K. (2014). GC skew and mitochondrial origins of replication. *Mitochondrion* 17, 56–66. doi: 10.1016/j.mito.2014.05.009

Sato, C., Nendai, N., Nagata, N., Okuzaki, Y., Ikeda, H., Minamiya, Y., et al. (2023). Origin and diversification of pheretimoid megascolecid earthworms in the Japanese Archipelago as revealed by mitogenomic phylogenetics. *Mol. Phylogenet. Evol.* 182, 107735. doi: 10.1016/j.ympev.2023.107735

Sha, Z. L., and Ren, X. Q. (2015). A new species of the genus Arcoscalpellum (Cirripedia, Thoracica, Scalpellidae) from deep waters in the South China Sea. *Chin. J. Oceanol. Limnol.* 33, 732–734. doi: 10.1007/s00343-015-4164-0

Shen, X., Tsang, L. M., Chu, K. H., Achituv, Y., and Chan, B. K. K. (2015). Mitochondrial genome of the intertidal acorn barnacle Tetraclita serrata Darwin 1854 (Crustacea: Sessilia): gene order comparison and phylogenetic consideration within Sessilia. *Mar. Genomics* 22, 63–69. doi: 10.1016/j.margen.2015.04.004

Shinozaki, K., and Yamaguchi-Shinozaki, K. (2000). Molecular responses to dehydration and low temperature: differences and cross-talk between two stress signaling pathways. *Curr. Opin. Plant Biol.* 3, 217–223. doi: 10.1016/S1369-5266(00)80068-0

Si, M. R., Li, Y. D., Jiang, S. G., Yang, Q. B., Jiang, S., Yang, L. S., et al. (2022). Identification of multifunctionality of the PmE74 gene and development of SNPs associated with low salt tolerance in Penaeus monodon. *Fish. Shellfish. Immunol.* 128, 7–18. doi: 10.1016/j.fsi.2022.07.010

Siebenaller, J. (2000). The effects of hydrostatic pressure on signal transduction in brain membranes of deep-sea fishes of the genus Coryphaenoides. *Fish. Physiol. Biochem.* 23, 99–106. doi: 10.1023/A:1007830722804

Simão, F. A., Waterhouse, R. M., Ioannidis, P., Kriventseva, E. V., and Zdobnov, E. M. (2015). BUSCO: assessing genome assembly and annotation completeness with single-copy orthologs. *Bioinformatics* 31, 3210–3212. doi: 10.1093/bioinformatics/btv351

Snieckute, G., Genzor, A. V., Vind, A. C., Ryder, L., Stoneley, M., Chamois, S., et al. (2022). Ribosome stalling is a signal for metabolic regulation by the ribotoxic stress response. *Cell. Metab.* 34, 2036–2046. doi: 10.1016/j.cmet.2022.10.011

Song, Y. J., and Yoon, J. M. (2013). Genetic differences of three *Pollicipes mitella* populations identified by PCR analysis. *Dev. Reprod.* 17, 199. doi: 10.12717/DR.2013.17.3.199

Srivastava, A., Barth, E., Ermolaeva, M. A., Guenther, M., Frahm, C., Marz, M., et al. (2020). Tissue-specific gene expression changes are associated with aging in mice. *Genomics Proteomics. Bioinf.* 18, 430–442. doi: 10.1016/j.gpb.2020.12.001

Stoneley, M., Harvey, R. F., Mulroney, T. E., Mordue, R., Jukes-Jones, R., Cain, K., et al. (2022). Unresolved stalled ribosome complexes restrict cell-cycle progression after genotoxic stress. *Mol. Cell.* 82, 1557–1572. doi: 10.1016/j.molcel.2022.01.019

Stradal, T. E., and Scita, G. (2006). Protein complexes regulating Arp2/3-mediated actin assembly. *Curr. Opin. Cell. Biol.* 18, 4–10. doi: 10.1016/j.ceb.2005.12.003

Suico, M. A., Shuto, T., and Kai, H. (2017). Roles and regulations of the ETS transcription factor ELF4/MEF. *J. Mol. Cell Biol.* 9, 168–177. doi: 10.1093/jmcb/mjw051

Sun, Y., Wang, M. X., Zhong, Z. S., Chen, H., Wang, H., Zhou, L., et al. (2022). Adaption to hydrogen sulfide-rich environments: Strategies for active detoxification in deep-sea symbiotic mussels, *Gigantidas platifrons*. Sci. *Total. Environ.* 804, 150054. doi: 10.1016/j.scitotenv.2021.150054

Thubaut, J., Puillandre, N., Faure, B., Cruaud, C., and Samadi, S. (2013). The contrasted evolutionary fates of deep-sea chemosynthetic mussels (Bivalvia, Bathymodiolinae). *Ecol. Evol.* 3, 4748–4766. doi: 10.1002/ece3.749

Timón-Gómez, A., Nývltová, E., Abriata, L. A., Vila, A. J., Hosler, J., and Barrientos, A. (2018). Mitochondrial cytochrome c oxidase biogenesis: Recent developments. *Semin. Cell. Dev. Biol.* 76, 163–178. doi: 10.1016/j.semcdb.2017.08.055

Wang, P. P., Mao, Y., Su, Y. Q., and Wang, J. (2021). Comparative analysis of transcriptomic data shows the effects of multiple evolutionary selection processes on codon usage in *Marsupenaeus japonicus* and *Marsupenaeus pulchricaudatus*. BMC. *Genomics* 22, 1–14. doi: 10.1186/s12864-021-08106-y

Wang, J. L., Tong, C. W., Chang, W. T., and Huang, A. M. (2013). Novel genes FAM134C, C3orf10 and ENOX1 are regulated by NRF-1 and differentially regulate neurite outgrowth in neuroblastoma cells and hippocampal neurons. *Gene* 529, 7–15. doi: 10.1016/j.gene.2013.08.006

Waterhouse, A., Bertoni, M., Bienert, S., Studer, G., Tauriello, G., Gumienny, R., et al. (2018). SWISS-MODEL: homology modelling of protein structures and complexes. *Nucleic. Acids Res.* 46, W296–W303. doi: 10.1093/nar/gky427

Wei, L., He, J., Jia, X., Qi, Q., Liang, Z. S., Zheng, H., et al. (2014). Analysis of codon usage bias of mitochondrial genome in Bombyx mori and its relation to evolution. *BMC. Evol. Biol.* 14, 262. doi: 10.1186/s12862-014-0262-4

Wei, H. M., Hu, J., Pu, J., Tang, Q. L., Li, W. C., Ma, R. H., et al. (2019). Long noncoding RNA HAGLROS promotes cell proliferation, inhibits apoptosis and enhances autophagy via regulating miR-5095/ATG12 axis in hepatocellular carcinoma cells. *Int. Immunopharmacol.* 73, 72–80. doi: 10.1016/j.intimp.2019.04.049

Wei, Z. Y., Wen, Q., Li, W. R., Yuan, X. Q., Fu, Q. L., Cui, Z. W., et al. (2021). ATG12 is involved in the antiviral immune response in large yellow croaker (*Larimichthys crocea*). *Fish. Shellfish. Immunol.* 119, 262–271. doi: 10.1016/j.fsi.2021.10.015

Wilhelm, B. T., and Landry, J. R. (2009). RNA-Seq—quantitative measurement of expression through massively parallel RNA-sequencing. *Methods* 48, 249–257. doi: 10.1016/j.ymeth.2009.03.016

Xin, Q., Hui, M., Li, C. L., and Sha, Z. L. (2021). Eyes of differing colors in *Alvinocaris longirostris* from deep-sea chemosynthetic ecosystems: genetic and molecular evidence of its formation mechanism. *J. Oceanol. Limnol.* 39, 282–296. doi: 10.1007/s00343-020-9312-5

Yan, G. Y., Lan, Y., Sun, J., Xu, T., Wei, T., and Qian, P. Y. (2022). Comparative transcriptomic analysis of in *situ* and onboard fixed deep-sea limpets reveals sample preparation-related differences. *iScience* 25, 104092. doi: 10.1016/j.isci.2022.104092

Yan, G. Y., Sun, J., Wang, Z. S., Qian, P. Y., and He, L. S. (2020). Insights into the synthesis, secretion and curing of barnacle cyprid adhesive via transcriptomic and proteomic analyses of the cement gland. *Mar. Drugs* 18, 186. doi: 10.3390/md18040186

Yoon, M., Jung, J. Y., and Kim, D. S. (2013). Genetic diversity and gene flow patterns in *Pollicipes mitella* in Korea inferred from mitochondrial DNA sequence analysis. *Fish. Aquatic. Sci.* 16, 243–251. doi: 10.5657/FAS.2013.0243

Yu, P., Zhou, L., Zhou, X. Y., Yang, W. T., Zhang, J., Zhang, X. J., et al. (2019). Unusual AT-skew of *Sinorhodeus microlepis* mitogenome provides new insights into mitogenome features and phylogenetic implications of bitterling fishes. *Int. J. Biol. Macromol.* 129, 339–350. doi: 10.1016/j.ijbiomac.2019.01.200

Yuan, Y., Huang, Y., Jian, J., Cai, S., and Yang, S. (2022). Autophagy genes of ATG5-ATG12 complex in response to exogenous stimulations in *Litopenaeus vannamei*. *Isr. J. Aquacult-Bamid.* 74, 17. doi: 10.46989/001c.55792

Zhang, C., Zhang, Q., Pang, Y., Song, X., Zhou, N., and Wang, J. (2019). The protective effects of melatonin on oxidative damage and the immune system of the Chinese mitten crab (*Eriocheir sinensis*) exposed to deltamethrin. *Sci. Total Environ.* 653, 1426–1434. doi: 10.1016/j.scitotenv.2018.11.063

Zhang, B., Zhang, Y. H., Wang, X., Zhang, H. X., and Lin, Q. (2017). The mitochondrial genome of a sea anemone Bolocera sp. exhibits novel genetic structures potentially involved in adaptation to the deep-sea environment. *Ecol. Evol.* 7, 4951–4962. doi: 10.1002/ece3.3067

Zheng, P., Wang, M. X., Li, C. L., Sun, X. Q., Wang, X. C., Sun, Y., et al. (2017). Insights into deep-sea adaptations and host–symbiont interactions: A comparative transcriptome study on Bathymodiolus mussels and their coastal relatives. *Mol. Ecol.* 26, 5133–5148. doi: 10.1111/mec.14160

Zhou, L., Li, M. N., Zhong, Z. S., Chen, H., Wang, X. C., Wang, M. X., et al. (2021). Biochemical and metabolic responses of the deep-sea mussel Bathymodiolus platifrons to cadmium and copper exposure. *Aquat. Toxicol.* 236, 105845. doi: 10.1016/j.aquatox.2021.105845

Zhou, Y. D., Zhang, D. S., Zhang, R. Y., Liu, Z. S., Tao, C. H., Lu, B., et al. (2018). Characterization of vent fauna at three hydrothermal vent fields on the Southwest Indian Ridge: implications for biogeography and interannual dynamics on ultraslow-spreading ridges. *Deep. Sea. Res. 1. Oceanogr. Res. Pap.* 137, 1–12. doi: 10.1016/j.dsr.2018.05.001